Cell Reports, Volume *9*

Supplemental Information

Uncoupling Malt1 Threshold Function from Paracaspase Activity Results in Destructive Autoimmune Inflammation

Andreas Gewies, Oliver Gorka, Hanna Bergmann, Konstanze Pechloff, Franziska Petermann, Katharina M. Jeltsch, Martina Rudelius, Mark Kriegsmann, Wilko Weichert, Marion Horsch, Johannes Beckers, Wolfgang Wurst, Mathias Heikenwalder, Thomas Korn, Vigo Heissmeyer, and Jürgen Ruland

Inventory of Supplemental Information

Supplemental information include three supplemental figures (Figures S1–S3), Supplemental Experimental Procedures and Supplemental References.

Figure S1
Generation of Malt1 paracaspase mutant mice.
Related to Supplemental Experimental Procedure “Generation of *Malt1* paracaspase mutant (PM) knock-in mice”

Figure S2
Phenotypic analysis of *Malt1*$^{PM/-}$, *Malt1*$^{PM/PM}$ and *Malt1*$^{PM/+}$ animals.
Related to Fig. 1

Figure S3
Cleavage of Malt1 targets in T cells from *Malt1*$^{+/-}$, *Malt1*$^{PM/-}$ and *Malt1*$^{-/-}$ mice.
Related to Fig. 5

Supplemental Experimental Procedures

Supplemental References

Figure S1

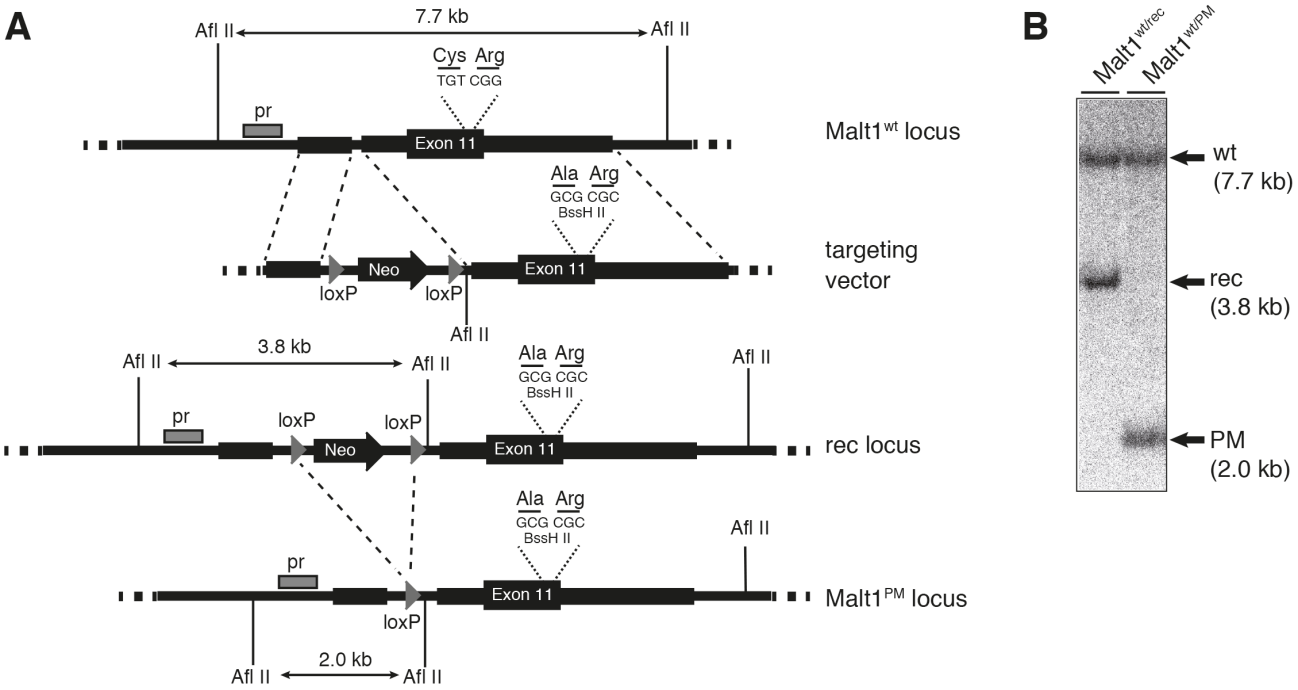

Figure S1 -
related to Supplemental Experimental Procedure "Generation of *Malt1* paracaspase mutant (PM) knock-in mice":

Generation of Malt1 paracaspase mutant mice. (A) Targeting strategy for homologous recombination at the *Malt1* genomic locus. The exon 11 region is shown, indicating the restriction fragment lengths produced by Afl II in the wild-type (wt), recombinant (rec), or PM allele that could be analyzed by Southern blotting using the probe (pr) marked in grey. The targeting vector contains the terminal homology arms indicated by thick lines, exon 11 with the cysteine (TGT) to alanine (GCG) mutation in codon 472 and a silent mutation in codon 473 (CGG → CGC) generating an artificial BssH II site. The neomycin (Neo) selection cassette is flanked by loxP sites (grey triangles). Homologous recombination in ES cells produced the rec locus containing the mutated exon 11 and the loxP flanked Neo cassette. Crossing the rec allele in mice to cre deleter mice led to the removal of the Neo cassette and thus to the generation of the PM allele. **(B)** Southern blot validation of the wild-type (wt), recombinant (rec), and paracaspase mutant (PM) Malt1 alleles generated by homologous recombination of the *Malt1* locus. AflII-digested genomic DNA isolated from *Malt1*$^{wt/rec}$ thymi demonstrated the presence of the expected 7.7-kb wt fragment and the 3.8-kb rec fragment. Deletion of the neomycin (Neo) resistance cassette yielded the *Malt1*$^{wt/PM}$ genotype (also named *Malt1*$^{PM/+}$ within this manuscript) which was confirmed by detecting the expected PM fragment at 2.0 kb.

Figure S2

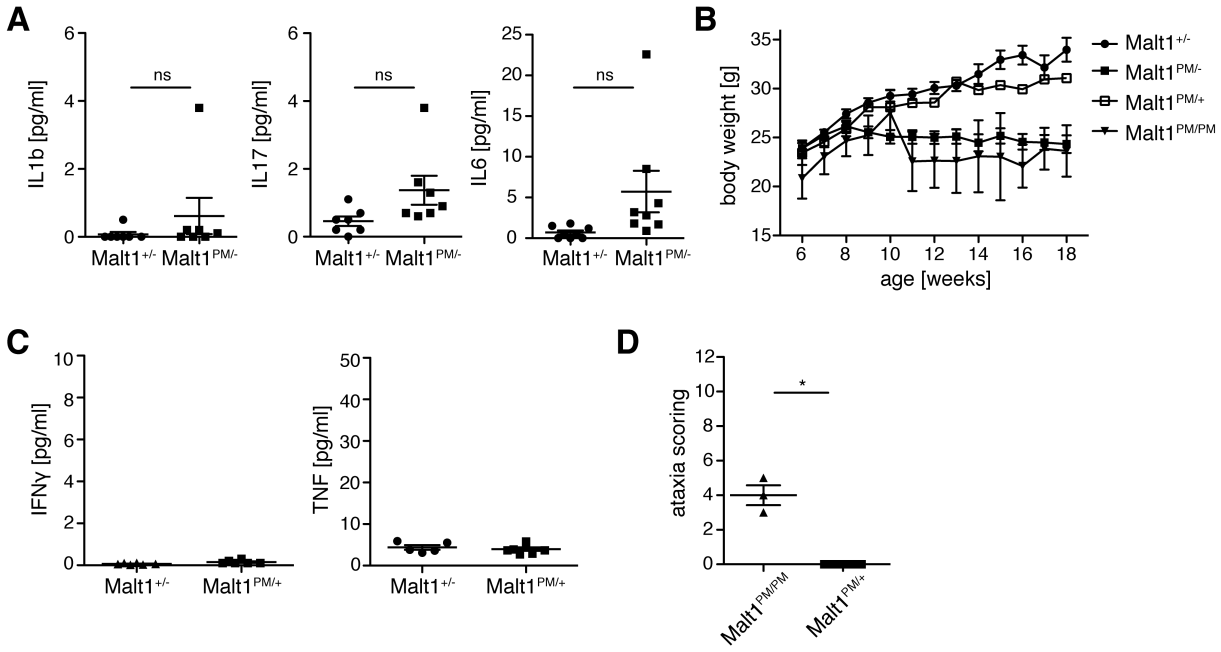

Figure S2 –
related to Fig. 1:

Phenotypic analysis of *Malt1*$^{PM/-}$, *Malt1*$^{PM/PM}$ and *Malt1*$^{PM/+}$ animals. (A) Serum concentrations of IL-1β, IL-17, and IL-6 were measured for *Malt1*$^{+/-}$ (n=7) and *Malt1*$^{PM/-}$ (n=7-8) mice at an age of 6 to 10 weeks. Horizontal bars indicate the means ± SEM (two-tailed unpaired t-test). **(B)** Body weight curves for *Malt1*$^{PM/+}$ and *Malt1*$^{PM/PM}$ mice were compared to those of *Malt1*$^{+/-}$ and *Malt1*$^{PM/-}$ mice (n>3 per time point, means ± SEM). **(C)** IFNγ and TNF levels in the serum of *Malt1*$^{+/-}$ (n=5) and *Malt1*$^{PM/+}$ (n=5) animals at 3-5 months of age. Horizontal bars indicate the means ± SEM (two-tailed unpaired t-test). **(D)** Ataxia scoring of *Malt1*$^{PM/PM}$ (n=3), and *Malt1*$^{PM/+}$ (n=6) at an age of 4 -5 months. Horizontal bars indicate the means ± SEM, Mann-Whitney test. * $P < 0.05$, ns = not significant.

Figure S3

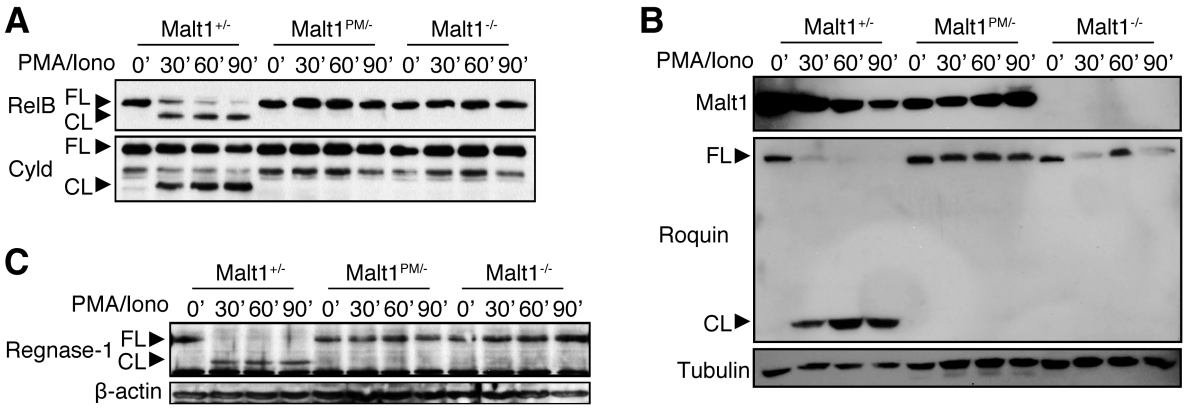

Figure S3 –
related to Fig. 5:

Cleavage of Malt1 targets in T cells from *Malt1*$^{+/-}$, *Malt1*$^{PM/-}$ and *Malt1*$^{-/-}$ mice. (A) CD4+ T cells from *Malt1*$^{+/-}$, *Malt1*$^{PM/-}$, and *Malt1*$^{-/-}$ mice were stimulated with PMA and ionomycin for the indicated time points in the presence of the proteasome inhibitor MG132. Cell lysates were analyzed by immunoblot using antibodies to RelB and Cyld. **(B, C)** CD4+ T cells from *Malt1*$^{+/-}$, *Malt1*$^{PM/-}$, and *Malt1*$^{-/-}$ mice were stimulated as in (A) and analyzed by immunoblot using specific antibodies to Malt1, Roquin1/2, and tubulin (B) or Regnase-1 and β-actin (C).

Supplemental Experimental Procedures

Generation of *Malt1* paracaspase mutant (PM) knock-in mice. A 715 bp fragment within intron 10 of the *Malt1* gene was used as a short arm (SA) for homologous recombination, and a 5.6 kb sequence downstream of the SA including exon 11 with the mutated nucleotide stretch TGTCGG (Cys-Arg) → GCGCGC (Ala-Arg) at codons 472+473 was used as a long arm (LA) for homologous recombination (see Figure S1 A). SA and LA were cloned into the pSPUC-DTA targeting vector which then was electroporated into E14tg2A.4 ES cells according to standard procedures. Cre deleter mice (Jax human CMV-Cre deleter strain B6.C-Tg(CMV-cre)1Cgn/J) were used to remove the Neo cassette. The *Malt1*^{PM} allele was back crossed to the C57bl/6J background for at least 8 generations (N8), all other mouse strains used in this study were also in a C57bl/6 background. *Malt1*$^{PM/+}$ mice were crossed with *Malt1*$^{-/-}$ mice (Ruland et al., 2003) to compare mice with a paracaspase mutant allele (Malt1$^{PM/-}$) to control animals with wt Malt1 (*Malt1*$^{+/-}$) or to Malt1-deficient (*Malt1*$^{-/-}$) mice. As indicated in the text, the *Malt1*$^{PM/-}$ alleles were also crossed to *Bcl10*$^{-/-}$ mice (Ruland et al., 2001), *Rag1*$^{-/-}$ mice (B6.129S7-Rag1^{tm1Mom}/J) and *IFNg*$^{-/-}$ mice (B6.129S7-Ifng^{tm1Ts}/J). Mice were housed in a specific pathogen-free facility according to the FELASA recommendations (http://www.felasa.eu).

Genotyping PCR and Southern blotting. To distinguish the wild-type *Malt1* paracaspase allele from the PM allele, the following primers were used: fwd: 5'-ctggtggcacacactttag -3' and rev: 5'-ccaacatacatacgaatggac-3', which produce a 160 bp band for the paracaspase wt allele and a 340 bp band for the PM allele. To distinguish the *Malt1* wt from the ko (-) allele, the following primer set was used: fwd: 5'-actttcatcttgccagcactctttctta-3', wt rev: 5'-ctgctgctgacatgctacaatatgctg-3' or ko rev: 5'-gggtgggattagataaatgcctgctc, which produce a 500 bp band for the wt allele and a 400 bp band for the knockout allele. Southern hybridization was performed according to standard protocols.

Flow cytometry. To quantify cell populations by flow cytometry, single cell suspensions were stained with fluorochrome-labeled antibodies directed against CD4

(GK1.5), CD8a (53-6.7), B220 (RA3-6B2), CD19 (eBio1D3), TCRβ (H57-597), IgM (II/41), CD21 (7G6), CD23 (B3B4), CD25 (PC61.5), CD62L (MEL-14), CD44 (IM7), CD69 (H1.2F3), Foxp3 (FJK-16s) and CD16/CD32 (clone 93) all obtained from eBioscience or BD Biosciences. For intracellular staining, cells were fixed and permeabilized with a Foxp3 staining kit (eBioscience). For proliferation assays, MACS-bead purified CD4+ T cells were labeled with 2.5 μM carboxyfluorescein succinimidyl ester (CFSE) for 10 min at 37°C and subsequently incubated for the indicated times at 37°C. For survival assays, cells were stained with Annexin V and 7-AAD in Annexin V staining buffer (both eBioscience). Analyses of cell populations and proliferation were performed by flow cytometry in a FACSCantoII (BD). Immune populations in the brain were determined as described previously (Rothhammer et al., 2011).

Histology and immunohistochemistry. Organs were formalin-fixed, paraffin-embedded and cut (2 μm) before tissue sections were stained with HE. For immunohistochemical staining of Purkinje cells in the cerebella, an anti-calbindin antibody (ab1778, Abcam) was used with the Ventana i-view system. Images were acquired using either an Olympus BX53 microscope and CellSens Dimension Software or an AxioVert (Zeiss) microscope with an AxioCam and processed by AxioVision software (Carl Zeiss). Hematoxylin and eosin (HE) stained gastric tissue sections from all mice were evaluated by a pathologist (MK) according to the updated Sydney classification (Dixon et al., 1996) in order to determine the inflammatory activity in the gastric antrum. Grading of active and chronic inflammation was combined into an overall four-tier semiquantitative score (0=no inflammation, 1=mild inflammation, 2=moderate inflammation, 3=strong inflammation).

DSS colitis. At 8 weeks of age mice were treated with 3.5% DSS in their drinking water for 5 days and sacrificed on day 9 at the peak of colitis. The bodyweights of the animals were monitored daily, and the animals were euthanized if their bodyweights dropped by 20% of the initial body weight. The severity of DSS colitis in the mice was assessed by scoring the most affected area of each mouse from HE-stained formalin-fixed paraffin-embedded colon sections on a scale from 1-12. Scoring was

determined by criteria of immune cell infiltration, edema, epithelial damage and hyperplasia (Okayasu et al., 1990).

Immunization. Eight to nine-week-old mice were immunized intraperitoneally (i.p.) with 200 µl of $KAl(SO_4)_2*12H_2O$ (f.c. 5% (w/v), Sigma) precipitated nitrophenyl (NP)(18) ovalbumin (OVA) (f.c 0.5 mg/ml, Biosearch Technologies). NP-specific serum IgM and IgG1 concentrations were determined by ELISA applying the SBA Clonotyping™ System-AP and Mouse Immunoglobulin Panel (SouthernBiotech).

Immunoblot analysis. Cells were lysed in CHAPS lysis buffer (20 mM Tris·Cl pH 7.5, 150 mM NaCl, 1% CHAPS) after addition of protease inhibitor cocktail (Sigma). Immunoblot analysis was performed according to standard protocols. Antibodies from Cell Signaling
Technology were used to detect p-Erk (#9101), p-JNK (#9251), p-p38 (#9211), p-IKKa/IKKb (#2697), IkBa (#9242), p-IkBa (#9246), RelB (#4922) and p-Atf2 (#5112), otherwise Cyld (E-10, Santa Cruz), Regnase-1 (clone 604421**,** R&D), Roquin (clone 3F12 provided by V. Heissmeyer), Malt1 (Ruefli-Brasse et al., 2003), Gapdh (Calbiochem, CB1001), b-actin (A5060, Sigma) and Tubulin (sc-23948, Santa Cruz) were used.

NF-κB assays. Electromobility shift assays were performed as described (Ruland et al., 2001) and ELISA-based NF-κB binding assays were performed with nuclear extracts using the TransAM® NF-κB factor ELISA Kit (Active Motif). To detect p50, p52, RelB and p65 antibodies provided by the TransAM® kit were used; to detect cRel the sc-71 X antibody (Santa Cruz Biotechnology) was used.

qRT PCR analysis and RNA stability assay. For qRT PCR, total RNA was prepared using a combination of TRIzol extraction and subsequent column purification (RNeasy kit, Qiagen). cDNA was synthesized from total RNA using Superscript II Reverse Transcriptase (Life Technologies) with random primers. qPCR was performed using a LightCycler LC480 (Roche) and SYBR green from the qPCR Core kit (Eurogentec). To assay RNA stability, bead-purified CD4+ T-cells were

stimulated for four hours with PMA/ionomycin before transcription was blocked by the addition of actinomycin D (10 µg/ml) for the indicated time points. Total RNA isolation and qPCR were performed as described above. The following primers were used for qPCR: Ifng-fwd: ctgaataactattttaactcaagtg, Ifng-rev: gattttcatgtcaccatccttttg; Tnf-fwd: actccaggcggtgcctatg, Tnf-rev: gagcgtggtggcccct; and as a reference ActB-fwd: cacacccgccaccagttcg, ActB-rev: caccatcacaccctggtgc.

Microarray analysis. Naive CD4+ T cells (CD62L+ CD25-) were sorted using a MoFlo cell sorter (Beckman Coulter) and stimulated with 50 ng/ml plate-bound anti-CD3 (145-2C11) and 2 µg/ml anti-CD28 (37.51) antibodies after pre-coating with anti-Syrian hamster antibodies using a minimum of $3x10^6$ cells per time point in one well of a 6-well plate. Total RNA was isolated as described for the qRT PCR analysis, and the quality was validated by analysis with an Agilent Bioanalyzer. RNA was amplified using the Illumina TotalPrep RNA amplification kit (Ambion). The amplified cRNA was hybridized to MouseRef-8v2 Expression BeadChips (Illumina, San Diego) for 16 h. Staining and scanning were performed according to the Illumina expression protocol. Data were normalized using the GenomeStudio Version 2011.1 software and processed using quantile normalization, the background subtraction option, and the introduction of an offset to remove remaining negative expression values. Statistical analysis was performed with the TM4 software package, selecting significantly regulated genes with a fold change > 2 in combination with a FDR < 10%. The expression profiling data set was submitted to the GEO database (GSE55360, http://www.ncbi.nlm.nih.gov/geo/query/acc.cgi?token=ajsdwguspxcrvkf&acc=GSE55360). NF-kB target genes were defined according to the Gilmore laboratory at Boston University (http://www.bu.edu/nf-kb/gene-resources/target-genes/) and additional previous reports (Compagno et al., 2009).

Supplemental References

Compagno, M., Lim, W.K., Grunn, A., Nandula, S.V., Brahmachary, M., Shen, Q., Bertoni, F., Ponzoni, M., Scandurra, M., Califano, A.*, et al.* (2009). Mutations of multiple genes cause deregulation of NF-kappaB in diffuse large B-cell lymphoma. Nature *459*, 717-721.

Dixon, M.F., Genta, R.M., Yardley, J.H., and Correa, P. (1996). Classification and grading of gastritis. The updated Sydney System. International Workshop on the Histopathology of Gastritis, Houston 1994. The American Journal of Surgical Pathology *20*, 1161-1181.

Okayasu, I., Hatakeyama, S., Yamada, M., Ohkusa, T., Inagaki, Y., and Nakaya, R. (1990). A novel method in the induction of reliable experimental acute and chronic ulcerative colitis in mice. Gastroenterology *98*, 694-702.

Rothhammer, V., Heink, S., Petermann, F., Srivastava, R., Claussen, M.C., Hemmer, B., and Korn, T. (2011). Th17 lymphocytes traffic to the central nervous system independently of alpha4 integrin expression during EAE. The Journal of Experimental Medicine *208*, 2465-2476.